energies

MDPI

Article

Heuristic Optimization Approaches for Capacitor Sizing and Placement: A Case Study in Kazakhstan

Olzhas Baimakhanov [1], Hande Şenyüz [2], Almaz Saukhimov [1] and Oğuzhan Ceylan [3,*]

[1] Electrical Power Systems Department, Almaty University of Power Engineering & Telecommunications Named after G. Daukeyev, Almaty 480013, Kazakhstan; o.baimakhan@aues.kz (O.B.); a.saukhimov@aues.kz; (A.S.)
[2] Management Information Systems Department, Kadir Has University, Istanbul 34083, Turkey; hande.senyuz@stu.khas.edu.tr
[3] Electrical and Electronics Engineering Department, Marmara University, Istanbul 34854, Turkey
* Correspondence: oguzhan.ceylan@marmara.edu.tr

Abstract: Two methods for estimating the near-optimal positions and sizes of capacitors in radial distribution networks are presented. The first model assumes fixed-size capacitors, while the second model assumes controllable variable-size capacitors by changing the tap positions. In the second model, we limit the number of changes in capacitor size. In both approaches, the models consider many load scenarios and aim to obtain better voltage profiles by minimizing voltage deviations and active power losses. We use two recently developed heuristic algorithms called Salp Swarm Optimization algorithm (SSA) and Dragonfly algorithm (DA) to solve the proposed optimization models. We performed numerical simulations using data by modifying an actual distribution network in Almaty, Kazakhstan. To mimic various load scenarios, we start with the baseline load values and produce random variations. For the first model, the optimization algorithms identify the near-optimal positioning and sizes of fixed-size capacitors. Since the second model assumes variable-size capacitors, the algorithms also decide the tap positions for this case. Comparative analysis of the heuristic algorithms shows that the DA and SSA algorithms give similar results in solving the two optimization models: the former gives a slightly better voltage profile and lower active power losses.

Keywords: smart grid; optimization; capacitor allocation and sizing problem; heuristic methods

Citation: Baimakhanov, O.; Şenyüz, H.; Saukhimov, A.; Ceylan, O. Heuristic Optimization Approaches for Capacitor Sizing and Placement: A Case Study in Kazakhstan. *Energies* **2022**, *15*, 3148. https://doi.org/10.3390/en15093148

Academic Editor: Javier Contreras

Received: 23 February 2022
Accepted: 11 April 2022
Published: 26 April 2022

1. Introduction

The load and generation structure of distribution systems is changing. The integration of many renewable energy sources such as photovoltaics (PVs) and wind turbines (WTs), as well as the increasing number of electric vehicles (EVs) on roads around the globe, will impact distribution grids. In addition, deregulation has been implemented in almost every country in the world. These changes affect control strategies, planning efforts, and so on. The fluctuations caused by WTs and PVs can increase system losses and cause overvoltage and undervoltage problems. Moreover, the high number of EVs in the distribution grid may cause unexpected voltage drops if an appropriate coordinated operation strategy, including a grid-to-vehicle strategy and/or a vehicle-to-grid strategy, is not applied.

Conventional approaches to overcoming voltage problems include the use of bank capacitors and voltage regulators. As is well known, capacitors can provide reactive power to distribution systems. Thus, if capacitor bank locations are properly chosen and of sufficient size, they can help solve potential problems in distribution systems. Because these are mechanical devices, frequent changes in tap positions can reduce the life expectancy of the capacitors. To properly determine optimal sizes, mathematical models should consider distribution system power flows and physical device and/or system boundary constraints. Modeling the power flows of power distribution systems differs from those of power transmission systems because of the high R/X (R indicates the resistance of the line and

X denotes the reactance of the line) ratios in the former. Instead of the Newton–Raphson-based power flow method, the preferred approach is to use the Kirchhoff Law-based backward/forward sweep power flow model [1]. There have been numerous attempts to determine the locations and sizes of capacitors. As described in detail in [2], we can divide the solution methods into analytical methods, numerical methods, heuristic methods, and artificial intelligence-based methods. As far as we know, the first attempts were based on analytical calculations from the 1950s, a detailed analysis to determine optimal locations for capacitors assuming distributed loads with the goal of reducing power losses without considering voltage problems [3]. The authors of [4] solved an analytical derivative-based model and applied it to a 20-node system, and [5] improved on the idea. The analytical approach of [6] did not consider voltage regulation.

Later, numerical methods began to be used. From too numerous implementations, a first phase of the study was [7]; later methods focused on placement [8], and dimensioning [9] influenced the literature. One of the first numerical methods used to solve optimal capacitor placement was based on dynamic programming [10]. In [11], the Beale method, a modification of the simplex method, was used to solve the modeled quadratic problem. In [12,13], the authors propose solutions based on a nonlinear programming approach. In [14], the problem was first linearized, and then the solution approach was applied to the data of the distribution system of Caracas, Venezuela.

Several heuristic optimization algorithms have also been used to solve the capacitor location and size problem. The authors of [15] used Particle Swarm Optimization (PSO) in microgrids to calculate the best locations and sizes of capacitors. Considering the discrete nature of capacitors, the article [16] implemented the Cuckoo Search algorithm (CSA) to reduce annual costs and power losses. In [17], a 2-stage method for a 33-bus test system based on a genetic algorithm (GA) and PSO is proposed. In [18], using the ideas of chaotic search, opposition-based learning, and quantum physics, they improved the parameter selection process of the differential evolution technique [19]. They also improved the method by adding acceleration and migration operations and applying them to the capacitor placement problem. The cable thermal evaluation model [20] was used as an improved version of the capacitor optimal placement model using the Bacterial Aggregation Optimization (BAO) algorithm.

In addition, the influence of the load model on the optimal capacitor allocation and sizing was analyzed. In [21], the researchers used fuzzy set theory to select the most appropriate candidate solutions from a set of Pareto-optimal candidate solutions during the analysis of the capacitor placement problem and distributed generation as a multi-objective optimization problem with load uncertainties.

The authors of [22] tackled the optimum capacitor placement problem by dividing each month into time periods and used their impacts on system loss. In [23], researchers created a model that correctly assigns DGs and capacitors in distribution networks to improve performance. In [24], the authors applied optimal placement of capacitors in unbalanced distribution systems to decrease losses and control voltage magnitudes.

Several new optimization methods have recently been improved. For example, in [25], the grasshopper heuristic optimization algorithm (GOA) is used to find the best location and size for capacitors. To find the optimal sizes and locations for capacitors, DGs, and charging stations for electric vehicles, the authors of [26] used GOA in a fuzzy multi-objective model. A modified version of the Dragonfly algorithm [27] is used to optimally allocate capacitors and EV parking spaces [28] on a 33-bus distribution system. The authors of [29] proposed a model based on a Salp Swarm Optimization algorithm (SSA [30]) to find optimal locations for PVs and capacitors. Another study used the Moth–Flame Optimization (MFO) method to determine optimal locations for the 33-bus test system in [31].

This paper solves the problem of optimal placement and sizing of capacitors considering load variations by extending our earlier work [32]. We use two recently developed optimization algorithms, namely Salp Swarm Optimization algorithm and Dragonfly algorithm. SSA uses fewer parameters compared to other heuristic methods. It is an easily

applicable optimization algorithm that is powerful because of its searching abilities of the neighboring points [33]. Similar to SSA, the required control parameters are fewer compared to other algorithms in DA. DA is a memory-efficient algorithm with lower probability of falling into local optima [34].

Briefly, the contributions are given below:

- We model the problem of optimal capacitor placement and sizing considering load variations using fixed and variable capacitor sizes to minimize active power losses simultaneously.
- We use two recent heuristic approaches, namely the Dragonfly algorithm (DA) [27], and the Salp Swarm Optimization algorithm (SSA) [30] as tools to find the near-optimal locations and sizes of bank capacitors in distribution systems.
- We compare numerical simulation results obtained with heuristic methods.
- Actual distribution network data from Almaty, Kazakhstan, are used to evaluate the simulations.

The paper is structured as follows. In Section 2, we give the optimization models used to determine the optimal locations and sizes. Then, we explain the heuristic methods used and their applications to solve the optimization models. We solve the problem using the Almaty distribution system as an example, and illustrate the simulation results before concluding the paper.

2. Optimization Model

Two optimization models are used in this study, the first assuming that the capacitors used are of fixed size and the second that they are variable-size bank capacitors with different tap positions. The first optimization model aims to minimize the voltage deviations from the reference voltage (1 pu) and the active power losses simultaneously. In addition, the model considers different time points to simulate the different behavior of the load. The mathematical model of the first optimization model is as follows.

$$\begin{aligned} \text{minimize} \quad & \sum_{t=1}^{N_{\text{Time}}} \sum_{i=1}^{N_{\text{Bus}}} [(V_{it} - 1)^2] + \sum_{t=1}^{N_{\text{Time}}} P_{\text{loss}t} \\ \text{subject to} \quad & \text{Power flow constraints,} \\ & V_{it} \leq 1.05, \\ & V_{it} \geq 0.95, \\ & Cap_j \geq 25\,\text{kvar}, \quad j = 1, 2, \ldots, n, \\ & Cap_j \leq 400\,\text{kvar}, \quad j = 1, 2, \ldots, n, \\ & \text{Loc}_i \in \{2, 3, \ldots, \text{number of buses}\}, \quad \text{Loc}_i \neq \text{Loc}_j \end{aligned} \tag{1}$$

Please note that V_{it} is the voltage magnitude of node i at simulation time t, $P_{\text{loss}t}$ represents the sum of active power losses on all branches at the simulation time. The number of capacitors in the model is limited to n and cannot be installed on the first node, but can be installed on the following nodes. The capacitors' capacities are limited to between 25 and 400 per kvar. Furthermore, we try to limit the voltage magnitudes between the lower and upper voltage magnitudes: 0.95 pu–1.05 pu.

In the second optimization model, which we present below, the objective is again to obtain a voltage profile with lower deviations and fewer power losses. However, this model assumes that the reactive power provided through the bank capacitors can vary using m tap positions. The solution algorithm can determine the value of the capacitor at a given time according to the determined size; i.e., for a tap position of m, if the size is Cap, the reactive power injected is m. Please note that the model allows a limited total number of tap changes (K).

$$\begin{aligned}
\text{minimize} \quad & \sum_{t=1}^{N_{\text{Time}}} \sum_{i=1}^{N_{\text{Bus}}} [(V_{it}-1)^2] + \sum_{t=1}^{N_{\text{Time}}} P_{\text{loss}t} \\
\text{subject to} \quad & \text{Power flow constraints,} \\
& V_{it} \leq V_{\max}, \\
& V_{it} \geq V_{\min}, \\
& \text{Cap}_j \geq C_{\min},\ j = 1, 2, \ldots, n, \\
& \text{Cap}_j \leq C_{\max},\ j = 1, 2, \ldots, n, \\
& \text{Loc}_i \in \{2, 3, \ldots, \text{number of buses}\}, \quad \text{Loc}_i \neq \text{Loc}_j, \\
& Tap_m, \ni m \in \{0, 1, \ldots, M\}, \\
& \sum_{j=1}^{n} \sum_{t=1}^{N_{\text{time}}-1} \text{sign}[|\text{Tap}_j(t+1) - \text{Tap}_j(t)|] \leq K
\end{aligned} \tag{2}$$

In (2), we show the current tap as m, and maximum number of taps as M. The limitations of the number of tap operations is shown in the last expression of (2).

3. Optimization Approaches

In this section, the optimization approaches used in the study, namely the Dragonfly algorithm and the Salp Swarm Optimization algorithm, are briefly explained. Then, their implementations for solving the proposed optimization models are given.

3.1. Dragonfly Algorithm

Dragonfly behavior is imitated by DA. These creatures can create small swarms that fly in different directions in a search region, or larger swarms that carry out the entire search activity. The algorithm's primary notion is based on these two distinct behaviors, which are similar to exploration and exploitation.

The initial phase in DA, as with all other evolutionary algorithms, is to create candidate solutions. As a result, in the search space, a random population of dragonflies with n members each representing a variable is formed. After that, each potential solution's objective functions are evaluated, and the solutions are saved. The position of the dragonflies is updated according to the following expression in each iteration of the algorithm [27].

$$\Delta X_{t+1} = (sS_i + aA_i + cC_i + fF_i + eE_i) + w\Delta X_t \tag{3}$$

where separation, alignment, cohesion, and inertia weights are represented by s, a, c, and w, respectively. There are two additional coefficients, f and e, representing the food factor and the enemy factor, respectively. The method considers the individuals by specifying S_i, A_i, C_i, F_i, and E_i, which represent the separation, alignment, cohesion, food source, and enemy position of the enemy of the ith individual, respectively, and all of these factors are updated in each iteration [27]. The provided formula is used to calculate the separation.

$$S_i = -\sum_{j=1}^{N} X - X_j \tag{4}$$

where $X - X_j$ is the distance of the current individual to the neighboring individual. Please note that N indicates the number of neighbors.

Similarly, alignment is simply equivalent to:

$$A_i = \frac{\sum_{j=1}^{N} V_j}{N} \tag{5}$$

where V_j shows the velocity of the corresponding individual.

The term cohesion is represented as follows.

$$C_i = \frac{\sum_{j=1}^{N} X_j}{N} - X \tag{6}$$

The two most important behaviors are attraction to a food source and diversion from enemies. Mathematically they are equivalent to

$$F_i = X^+ - X \tag{7}$$

$$E_i = X^- - X \tag{8}$$

where X^+ and X^- are the food and enemy location, respectively.

One can determine the updated position vectors as follows.

$$X_{t+1} = X_t + \Delta X_{t+1} \tag{9}$$

If the dragonfly does not have at least one neighboring dragonfly in this situation, Levy flights are used to update the position vectors, causing dragonflies to fly throughout the search space in a random walk. Suppose the dragonfly does not have at least one neighboring dragonfly. In that case, Levy flights are used to update the position vectors, causing dragonflies to fly throughout the search space in a random walk. Detailed information on the calculation of Levy flight can be found in [27].

$$X_{t+1} = X_t + Levy(d)X_t \tag{10}$$

The termination criterion, which can be the maximum number of iterations, is checked once the locations have been updated. If it is met, the process is completed; otherwise, the objective function values are calculated. The flowchart of DA is provided in Figure 1.

DA Implementation on Capacitor Placement and Sizing Problem

The following is a quick description of the algorithm used to implement DA on the capacitor placement and sizing problem

1. Create initial solution candidates:

$$Pop = \begin{bmatrix} X_{1,1} & X_{1,2} & \cdots & X_{1,n} \\ X_{2,1} & X_{2,2} & \cdots & X_{2,n} \\ \cdots & \cdots & \cdots & \cdots \\ X_{m,1} & X_{m,2} & \cdots & X_{m,n} \end{bmatrix} \tag{11}$$

   where $X_{i,j}$ represents the value of a given variable. Please note that n is the number of variables we are looking for, which is two times the number of capacitors for optimization model 1, including sizes and locations. The capacitors' locations (nodes) are represented by the first half of the variables ($n/2$). The capacitor sizes are represented by the remaining ($n/2$) variables. For optimization model 2, we consider tap positions and their time instants. Thus, with five capacitors, the number of variables in model 2 is 5 for the number of capacitors, 5 for their locations, for each capacitor, five tap positions are added with four tap position changes, giving a total of 55. The number of search agents are shown by m, which is the row size of the population matrix.
2. Evaluate the objective function of the optimization model 1 given in Equation (1) for each of the candidate solutions, as well as the objective function of the optimization model 2 given in Equation (2) for each of the candidate solutions. It is important to note that to do this, the power flow must be used. We created a power flow code based on a backward–forward sweep algorithm and used it in the simulations [35].
3. Add some randomness to w, s, a, c, f and e, and update in each iteration and find S, A, C, F and E.

4. Create new vectors of position. Please note that in optimization model 1, the sizes of the capacitors are real numbers. However, the locations of the capacitors are integers. Therefore, we apply rounding in the optimization; we round these values to the nearest integer. If the upper or lower bounds are violated, they are brought back into the allowable range. We apply a similar rounding procedure in solving optimization model 2, where we use additional variables representing the tap positions of the bank capacitors and time instants of the changes in the capacitor positions. In the optimization process, these values are rounded to the nearest integer, and the numerical values are brought into the bounds using modular arithmetic.
5. If the stopping criterion is satisfied, or the preset maximum number of iterations is reached, stop; otherwise, continue from step 3.

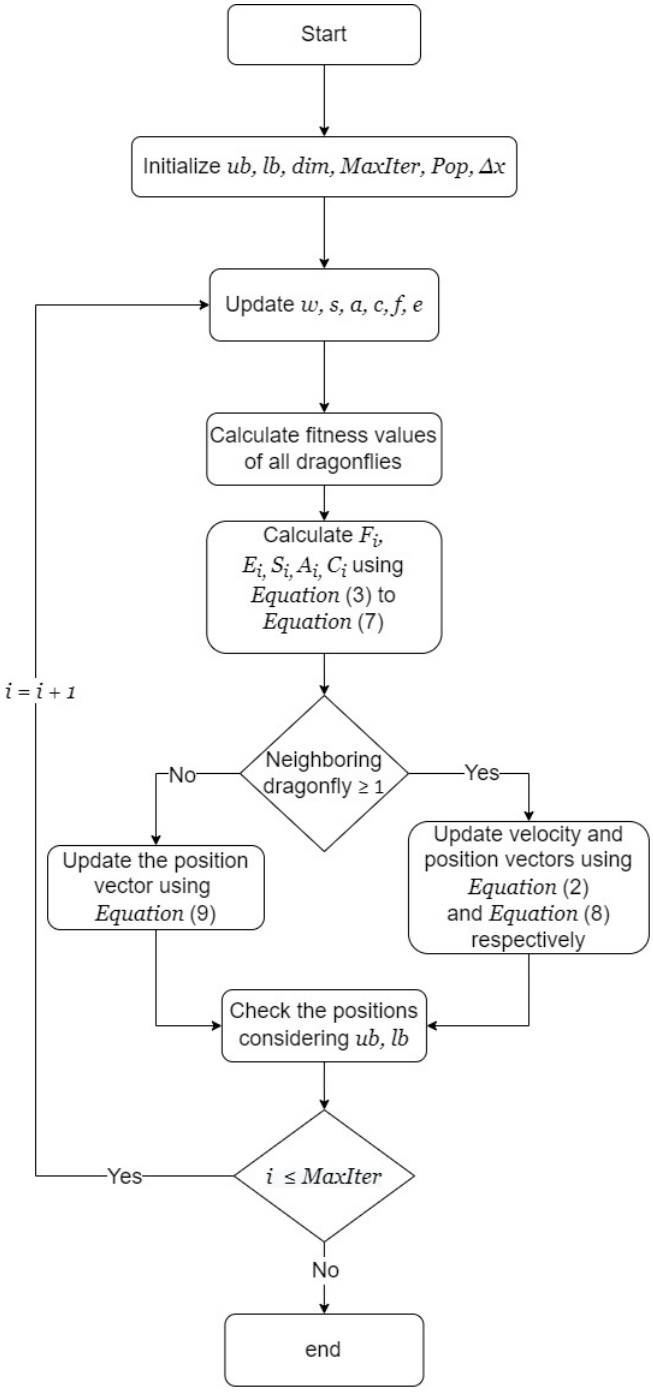

Figure 1. Flowchart of DA method.

3.2. Salp Swarm Optimization Algorithm

Salp Swarm Optimization algorithm mimics the swarming behavior of salps. A salp chain starts with a leader salp, and the follower salps exist in the rest of the chain. Therefore, there are two groups in the population—a leader and followers [30].

The algorithm initially creates solution candidates in the feasible solution space. Accordingly, for the n number of variables of a given problem, an n-dimensional search space is created for the initial position of salps. Then, the algorithm records the evaluated solutions of the salp population in a 2-dimensional matrix. The mathematical representation of solution updates of the leader salp is as follows (12):

$$x_j^1 = \begin{cases} F_j + c_1((ub_j - lb_j)c_2 + lb_j) & c_3 \geq 0 \\ F_j - c_1((ub_j - lb_j)c_2 + lb_j) & c_3 < 0 \end{cases} \tag{12}$$

where x_j^1, F_j, ub_j and lb_j represent leader salp position, food source position, upper bound and lower bound in the jth dimension, respectively. Other variables c_1, c_2 and c_3 are random numbers in the $[0, 1]$ interval. Please note that the updates of the leader salp position changes according to the food source. The parameter c_1 of the algorithm balances the exploration and exploitation behavior shown as below in Equation (13).

$$c_1 = 2e^{-(4l/L)^2} \tag{13}$$

where L and l show maximum iteration number and current iteration number, respectively.

The follower salps also update their positions. Equation (14) shows the updates for follower salps where x_j^i is the ith salp position in the jth dimension. Details about the calculation of motion of followers can be found in [30].

$$x_j^i = \frac{1}{2}x_j^i + x_j^{i-1} \tag{14}$$

The stopping condition is checked after position updates. If it is not met, the process is repeated from the evaluation of objective function values until the stopping criterion is met or the maximum number of iterations is reached. The flowchart of the SSA is given in Figure 2.

SSA Implementation on Capacitor Placement and Sizing Problem

The structure of the SSA implementation on the capacitor location and sizing problem is given below.

1. Initialize solution candidates of the population:

$$Pop = \begin{bmatrix} x_{1,1} & x_{1,2} & \cdots & x_{1,n} \\ x_{2,1} & x_{2,2} & \cdots & x_{2,n} \\ \cdots & \cdots & \cdots & \cdots \\ x_{m,1} & x_{m,2} & \cdots & x_{m,n} \end{bmatrix} \tag{15}$$

   As with the implementation of DA for solving optimization models, $x_{i,j}$ represents the value of a certain variable. As mentioned in the DA implementation, n is the number of variables that differ between optimization models 1 and 2. The number of search agents is represented by the size of the rows in the population matrix m.
2. Evaluate objective functions of (1) and (2) for each of the solution candidate for optimization model 1 and 2, respectively. We apply the backward–forward sweep algorithm-based power flow algorithm for this process [35].
3. Update c_1 and x^1, x^j by adding randomness in each iteration.
4. Calculate new position vectors by taking the integer values and their boundaries into consideration, similar to that explained for the implementation of DA.

5. If the stopping criterion is satisfied or the preset maximum number of iterations is reached, stop, otherwise continue from step 3.

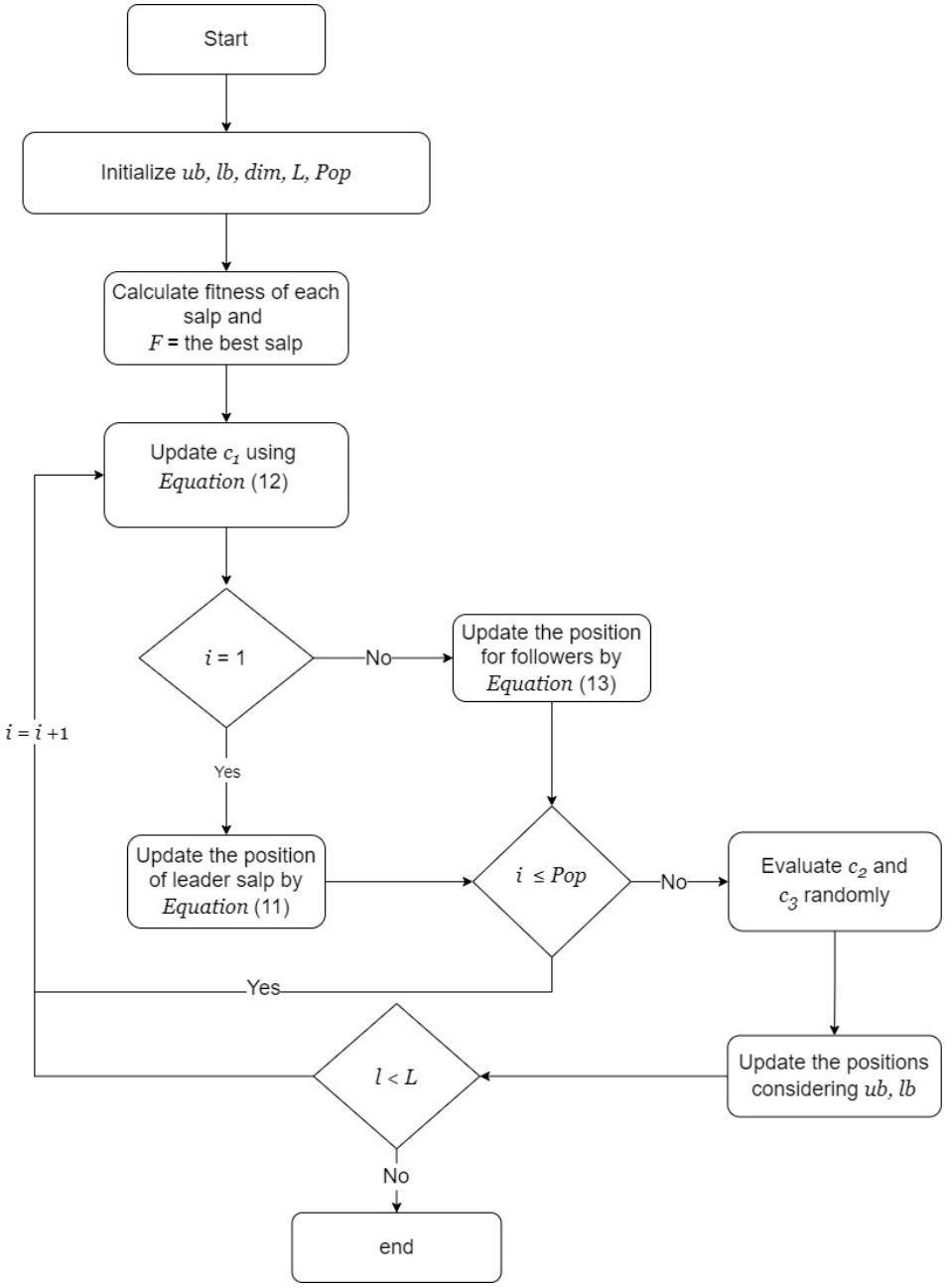

Figure 2. Flowchart of the SSA method.

4. Tests and Results

This section provides simulation results for the proposed two optimization models.

4.1. Test System and Data Preparation

To put the suggested optimization models to the test, we use the Almaty power network's actual radial 17-bus system. The grid data were given by the regional power utility JSC "AZhK". The purpose is to adjust the network's reactive power flow by using either fixed- or variable-size capacitors. To do this, we want to discover the best capacitor placement and size. Almaty's distribution network is divided into two sections, the first of which has 21 nodes and the second of which has 17 nodes. Assuming that the component with 17 nodes is a balanced system with a radial topology, as illustrated in Figure 3, to

mimic variations in the load profile over different time periods (i.e., changes over a day or days), we generated 1000 separate random load profiles by multiplying the artificially constructed load profile from [32]. We considered that the loads of all nodes may vary between 0.7 and 1.3 times the base case values to replicate load fluctuations throughout the day. Figure 4 depicts a sample of 20 randomly created multiplication rates for each node. For the branch reactance information, the reader may refer to [32].

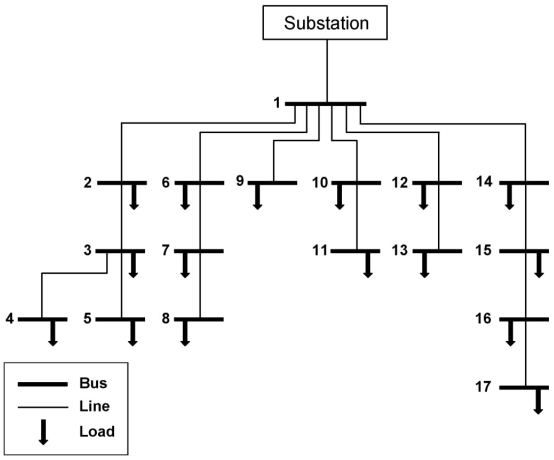

Figure 3. Single line diagram of Almaty 17-bus radial distribution network.

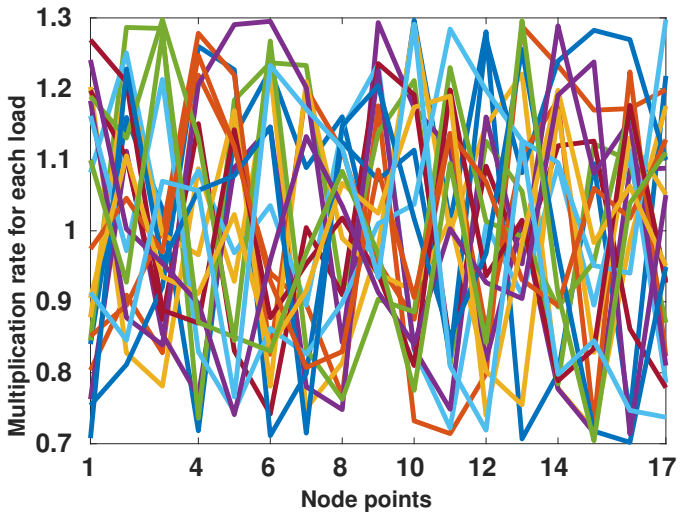

Figure 4. A sample of 20 randomly created multiplication rates for each of the base case loads.

4.2. Simulation Results

We applied the DA and SSA-based solution algorithms on an Intel(R) Core(TM) i7-9750H CPU @ 2.60 GHz computer. We used Matlab as a simulation tool to use SSA and DA toolboxes provided at [36,37] and solved the proposed optimization models.

4.3. Case 1: Fixed Capacitor Sizes

We used five capacitors with minimum and maximum capacities ranging from 25 to 400 kvar to solve the first optimization model. The capacitor placements and sizes are determined by the algorithms SSA and DA. For all simulations, we used 30 search agents and 500 iterations as the maximum number of iterations.

The first set of simulations aims to solve the problem of optimal sizing and placement of capacitors, where we assume fixed sizes of capacitors. As mentioned earlier, we consider a total of 1000 different loads. The summary of numerical simulation results obtained with SSA and DA algorithms can be found in Table 1 and Figure 5. Please note that the

near-optimal locations of the capacitors are determined as follows. Node numbers are 5, 14, 15, 16, and 17. For the specified nodes, the simulation finds the sizes as 400 kvar, 400 kvar, 400 kvar, 400 kvar, and 400 kvar, respectively.

We show the best and worst near-optimal solutions obtained using DA and SSA in Table 1, where DA(b) and SSA(b) represent the best near-optimal results obtained with SSA and DA, and DA(w) and SSA(w) represent the worst near-optimal results obtained with SSA and DA, respectively, from 100 different runs. From the presented results, the objective function values found for the best near-optimal solutions using two methods and thus the corresponding locations and sizes of the capacitors are the same. This is not the case for the worst near-optimal solutions. As can be observed from the table, the locations for the capacitors and their sizes are different from each other. Please note that in the table, the Method column represents the method used (i.e., DA or SSA), the Locations column represents the calculated near-optimal locations of the capacitors, the Sizes column represents the corresponding capacitor sizes, and the F column represents the value of the objective function.

Table 1. Best and worst simulation results obtained with SSA and DA for Case 1.

Method	Locations					Sizes (kvar)					F
DA (b)	5	14	15	16	17	400	400	400	400	400	324,917.31
DA (w)	7	14	15	16	17	267.12	289.74	376.83	343.84	400	336,775.59
SSA (b)	5	14	15	16	17	400	400	400	400	400	324,917.31
SSA (w)	11	14	15	16	17	74.38	109.19	400	400	400	338,625.19

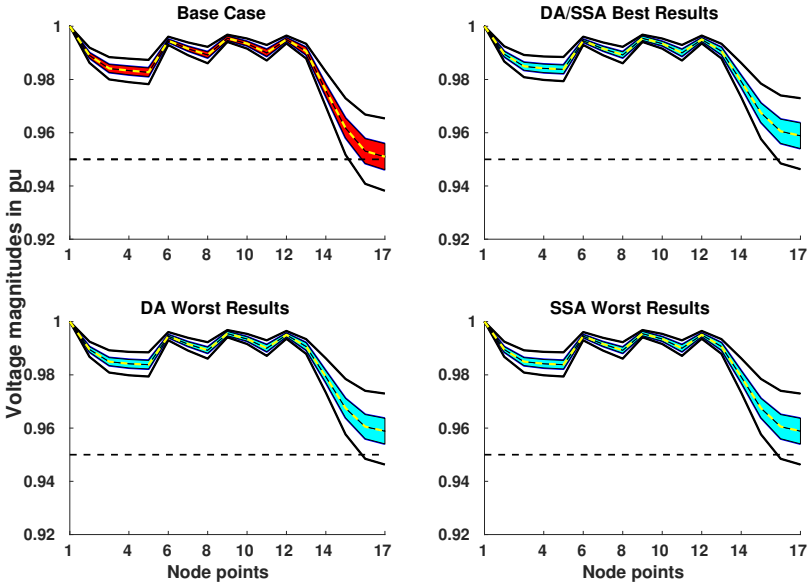

Figure 5. System voltage magnitudes before and after capacitor installments under various load scenarios.

In Figure 5, we illustrate the mean of the base case voltage magnitudes together with their standard deviations in the first part shown in red color. The remaining portions show the voltage magnitudes obtained with the best DA/SSA (results that provide the lowest objective function values) and the worst results obtained through DA and SSA runs. Please note that the improvement of the voltage profiles is evident even in the worst-case results for both methods. Moreover, the figure shows the maximum and minimum voltage magnitudes obtained with different results, and the shaded areas in the figures show the standard deviation from the mean voltage magnitude for a single solution. It is easy to see that the number of simulations leading to undervoltage problems is higher before the capacitors with their near-optimal sizes are installed in near-optimal locations than

after the capacitors are installed. If you look at the shaded areas, you will notice that the installation of capacitors also improves the standard deviations of the voltage magnitudes. We illustrate this in Figure 6 as well. For 100 simulations, the mean voltage magnitudes obtained with DA and SSA and their standard deviations are plotted in boxplot form. The figure shows that base case mean voltage magnitudes and their standard deviations are worse than SSA and DA-based solutions. The simulation results of the DA-based solution are the same as that of the SSA-based solution in terms of the mean voltage magnitudes and are slightly better than that of the SSA-based solution in terms of the standard deviations.

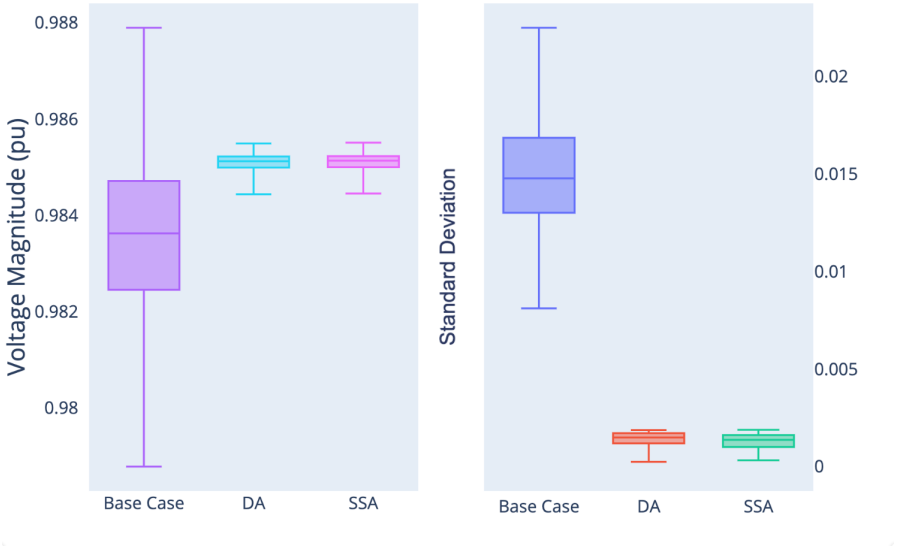

Figure 6. Mean voltage magnitudes and their standard deviations for base case, SSA and DA for Model 1.

Figure 7 illustrates the sorted active power losses for the base case and capacitor-installed configurations. The decrease of the active power losses when the capacitors are installed (for the best/worst near-optimal solutions obtained with SSA and DA-based algorithms) compared to the base case shown with a black line is evident in the figure. The slight differences in the active power losses of the best and worst configurations obtained with DA and SSA are illustrated. When the ideal location and size of the capacitors are identified, the losses are reduced.

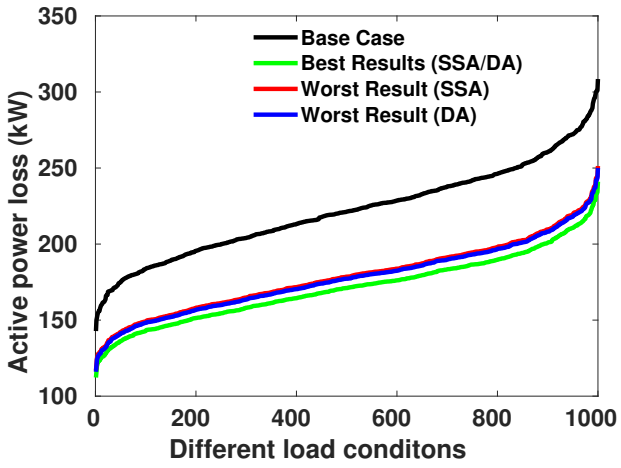

Figure 7. Active power losses of the distribution network considering different load conditions before and after capacitor installments (Case 1).

4.4. Case 2: Variable Capacitor Sizes through Tap Position Changes

We also performed simulations to solve the optimization problem given in the optimization model (2). As stated above, this case considers variable sizes for the capacitors. Similar to Case 1, we varied the loads and obtained 1000 different load profiles in the simulations. Different from Case 1, this case determines the sizes, locations, and the operating modes (different tap positions for the capacitors) for different load conditions.

We show the changes in the capacitor values over different load conditions for the best and worst solution cases obtained using SSA and DA-based algorithms in Figure 8. It can be seen from the figure that more successful results have higher capacitor values with nearly zero changes during the simulation period.

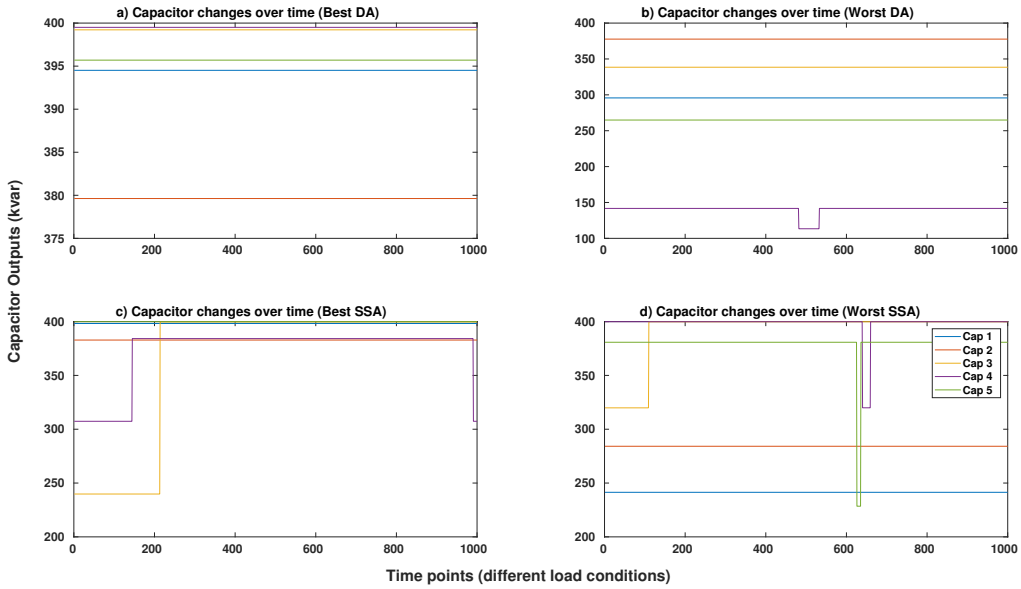

Figure 8. The changes of the capacitor values over time for SSA and DA-based algorithms: (**a**) Capacitor changes obtained with the best near-optimal result using DA, (**b**) Capacitor changes obtained with the worst near-optimal result using DA, (**c**) Capacitor changes obtained with the best near-optimal result using SSA, (**d**) Capacitor changes obtained with the worst near-optimal result using SSA.

Figure 9 shows the voltage magnitudes for the base case together with the best and worst solutions obtained from 100 different runs using SSA and DA-based algorithms. From the figure, as expected, better voltage profile may be obtained by adequately sizing, locating, and operating the capacitors using the solutions obtained by heuristic optimization approaches. As with Case 1, this case may still have a few under-voltages in very extreme cases (i.e., higher loads in the end nodes of the laterals).

The improvement of the voltage profile compared to the base case is shown in Figure 10. We illustrate the mean and standard deviation of the voltage magnitudes obtained with SSA and DA together with the base case magnitudes. In contrast to Case 1, this case provided slightly better mean voltage magnitudes and standard deviations using SSA-based algorithm compared to DA-based algorithm.

Figure 11 shows the active power loss values for the base case and capacitor-installed cases. We observe from the figure that, similar to Case 1, the decrease in the active power losses may draw attention compared to the base case. The best active power loss values are obtained with the best SSA solution configuration, which is slightly better than that of the best DA solution. When the ideal location and sizes of the capacitors were found, the losses were clearly reduced.

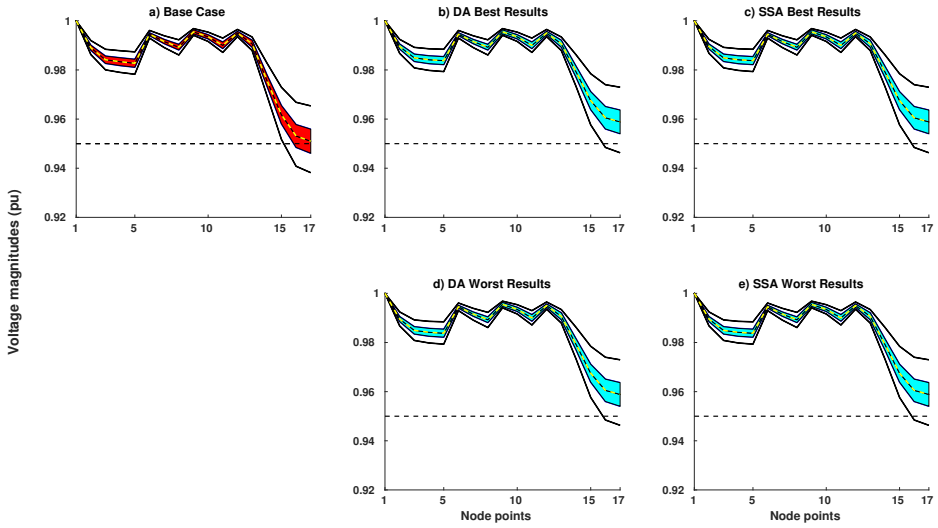

Figure 9. Voltage magnitudes after capacitor installments, (**a**) base case results, (**b**) best near-optimal results obtained with DA, (**c**) best near-optimal results obtained with SSA, (**d**) worst near-optimal results obtained with DA and (**e**) worst near-optimal results obtained with SSA.

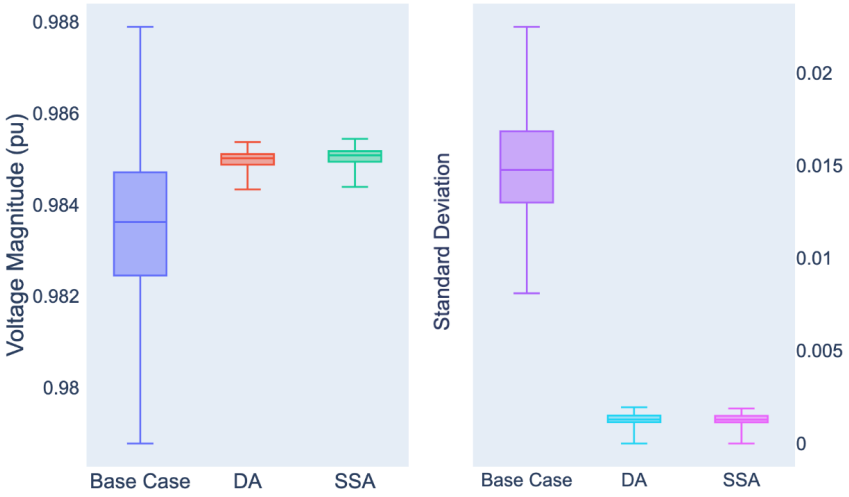

Figure 10. Mean voltage magnitudes and their standard deviations for base case, SSA and DA for Model 2.

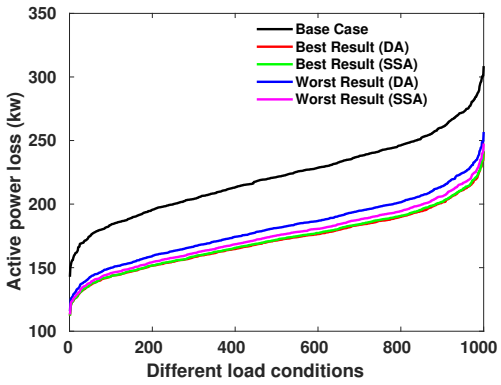

Figure 11. Active power losses of the distribution network considering different load conditions before and after capacitor installments (Case 2).

4.5. Comparison of the Results

We compared the performance of the results of the two optimization models. Table 2 shows the mean of the voltage magnitudes of solution of Cases 1 and 2. The overall mean of voltage magnitudes obtained with SSA and DA is given together with the base case mean voltage magnitude. From the table, we observe that SSA finds the best mean voltage magnitudes for Case 1 and Case 2, DA finds the same value for Case 1; however, for Case 2 it gives a slightly worse voltage magnitude.

Table 2. Mean of Voltage Magnitudes for Case 1 and 2.

V_{mean}			
Case 1		**Case 2**	
Base Case	0.9836	Base Case	0.9836
DA	0.9851	DA	0.9850
SSA	0.9851	SSA	0.9851

Table 3 shows the active power losses for 1000 different load conditions. We find from the table that the best case is obtained for Case 1 using DA and SSA. For Case 2, SSA provides a slightly better active power loss compared to DA. From these observations, we find that using a fixed-size capacitor provides slightly better results.

Table 3. Power Losses obtained for Case 1 and 2.

P_{loss}			
Case 1		**Case 2**	
Base Case	221,605.66	Base Case	221,605.66
DA	171,260.31	DA	171,505.18
SSA	171,260.31	SSA	171,427.63

5. Conclusions

In this paper, capacitor placement and sizing problems are solved using two recently developed heuristic optimization algorithms: DA and SSA. The optimization algorithms based on DA and SSA are implemented on two models to determine the optimal locations and sizes of capacitors. The first optimization model simultaneously minimizes the voltage deviations at each node and the total active power loss for several randomly generated different load conditions using fixed-size capacitors. The main difference between the first and second optimization models is the use of capacitors, which can provide different reactive power due to changes in the tap positions of the capacitors in the second optimization model. Additionally, the number of changes in the second optimization model is limited. In both optimization models, the size of the capacitors is assumed to be between 25 and 400 kvars. The models do not allow more than one capacitor to be installed at a single node. The tests were performed using the radial 17-bus system of Almaty, Kazakhstan, whose data were provided by the regional power utility. We varied each load in the 17-bus system in a range from 70% to 130% and created different load conditions. The simulations were performed assuming five capacitors with possible reactive powers ranging from 25 to 400 kvar. Voltage deviations and active power losses are reduced when capacitors are installed in near-optimal sizes and locations, according to the simulation results. The improvement of the voltage profile by solving the optimization problems is slightly different when different heuristics are used. This shows that both of the used heuristics (SSA, DA) can find near-optimal solutions. Due to the occurrence of undervoltage problems, especially in the most remote nodes of the laterals, the near-optimal solutions with variable and fixed-sized capacitors lead to similar voltage profiles and active power losses. In the experimental investigations carried out as part of this study, we also found

that better power loss values were obtained when fixed-size capacitors were used than when variable-size capacitors with a limited number of tap operations were used.

Author Contributions: Data curation, O.B. and H.Ş.; Formal analysis, O.B., H.Ş. and O.C.; Funding acquisition, A.S.; Investigation, O.B., H.Ş. and O.C.; Methodology, H.Ş., O.B. and O.C.; Project administration, A.S. and O.C.; Resources, O.B.; Software, O.B. and H.Ş.; Supervision, A.S. and O.C.; Validation, O.B. and H.Ş.; Visualization, O.B. and H.Ş.; Writing—original draft, O.B. and H.Ş.; Writing—review and editing, A.S. and O.C. All authors have read and agreed to the published version of the manuscript.

Funding: This paper has been produced within the framework funded under the Grant #AP08052770 "Optimization of planning and control of Smart Grid systems" (Contract No. 101 of 25 May 2020), supported by the Ministry of Education and Science of the Republic of Kazakhstan.

Institutional Review Board Statement: Not applicable.

Informed Consent Statement: Not applicable.

Data Availability Statement: Not applicable.

Conflicts of Interest: The authors declare no conflict of interest.

References

1. Eminoglu, U.; Hocaoglu, M. Distribution Systems Forward/Backward Sweep-based Power Flow Algorithms: A Review and Comparison Study. *Electr. Power Compon. Syst.* **2009**, *37*, 91–110. [CrossRef]
2. Aman, M.; Jasmon, G.; Bakar, A.; Mokhlis, H.; Karimi, M. Optimum shunt capacitor placement in distribution system—A review and comparative study. *Renew. Sustain. Energy Rev.* **2014**, *30*, 429–439. [CrossRef]
3. Neagle, N.M.; Samson, D.R. Loss Reduction from Capacitors Installed on Primary Feeders [includes discussion]. *Trans. Am. Inst. Electr. Eng. Part III Power Appar. Syst.* **1956**, *75*, 950–959. [CrossRef]
4. Cook, R.F. Optimizing the Application of Shunt Capacitors for Reactive-Volt-Ampere Control and Loss Reduction. *Trans. Am. Inst. Electr. Eng. Part III Power Appar. Syst.* **1961**, *80*, 430–441. [CrossRef]
5. Schmill, J.V. Optimum Size and Location of Shunt Capacitors on Distribution Feeders. *IEEE Trans. Power Appar. Syst.* **1965**, *84*, 825–832. [CrossRef]
6. Bae, Y.G. Analytical Method of Capacitor Allocation on Distribution Primary Feeders. *IEEE Trans. Power Appar. Syst.* **1978**, *PAS-97*, 1232–1238. [CrossRef]
7. Lee, S.H.; Grainger, J.J. Optimum Placement of Fixed and Switched Capacitors on Primary Distribution Feeders. *IEEE Trans. Power Appar. Syst.* **1981**, *PAS-100*, 345–352. [CrossRef]
8. Baran, M.E.; Wu, F.F. Optimal capacitor placement on radial distribution systems. *IEEE Trans. Power Deliv.* **1989**, *4*, 725–734. [CrossRef]
9. Baran, M.; Wu, F.F. Optimal sizing of capacitors placed on a radial distribution system. *IEEE Trans. Power Deliv.* **1989**, *4*, 735–743. [CrossRef]
10. Dura, H. Optimum Number, Location, and Size of Shunt Capacitors in Radial Distribution Feeders a Dynamic Programming Approach. *IEEE Trans. Power Appar. Syst.* **1968**, *PAS-87*, 1769–1774. [CrossRef]
11. Ertem, S. Optimal shunt capacitor sizing for reduced line loading, voltage improvement and loss reduction of distribution feeders. In Proceedings of the Twenty-First Annual North American Power Symposium, Rolla, MO, USA, 9–10 October 1989; pp. 262–269. [CrossRef]
12. Augugliaro, A.; Dusonchet, L.; Mangione, S. Optimal capacitive compensation on radial distribution systems using nonlinear programming. *Electr. Power Syst. Res.* **1990**, *19*, 129–135. [CrossRef]
13. Ertem, S.; Tudor, J.R. Optimal Shunt Capacitor Allocation by Nonlinear Programming. *IEEE Trans. Power Deliv.* **1987**, *2*, 1310–1316. [CrossRef]
14. Khodr, H.; Olsina, F.; Jesus, P.D.O.D.; Yusta, J. Maximum savings approach for location and sizing of capacitors in distribution systems. *Electr. Power Syst. Res.* **2008**, *78*, 1192–1203. [CrossRef]
15. Alexander, A.T.; Gonzalo Manuel, G.S.; Diego Luis, G.S.; Leony, O.M. Optimum location and sizing of capacitor banks using VOLT VAR compensation in micro-grids. *IEEE Lat. Am. Trans.* **2020**, *18*, 465–472.
16. Baysal, Y.A.; Altas, I.H. Cuckoo search algorithm for power loss minimization by optimal capacitor allocation in radial power systems. In Proceedings of the 2016 International Symposium on INnovations in Intelligent SysTems and Applications (INISTA), Sinaia, Romania, 2–5 August 2016; pp. 1–5.
17. Jafari, A.; Ganjeh Ganjehlou, H.; Khalili, T.; Mohammadi-Ivatloo, B.; Bidram, A.; Siano, P. A Two-Loop Hybrid Method for Optimal Placement and Scheduling of Switched Capacitors in Distribution Networks. *IEEE Access* **2020**, *8*, 38892–38906. [CrossRef]
18. Chiou, J.P.; Chang, C.F. Development of a novel algorithm for optimal capacitor placement in distribution systems. *Int. J. Electr. Power Energy Syst.* **2015**, *73*, 684–690. [CrossRef]

19. Storn, R.; Price, K. Differential Evolution—A Simple and Efficient Heuristic for global Optimization over Continuous Spaces. *J. Glob. Optim.* **1997**, *11*, 341–359. [CrossRef]
20. Othman, A.M. Optimal capacitor placement by Enhanced Bacterial Foraging Optimization (EBFO) with accurate thermal re-rating of critical cables. *Electr. Power Syst. Res.* **2016**, *140*, 671–680. [CrossRef]
21. Biswal, S.R.; Shankar, G. Simultaneous optimal allocation and sizing of DGs and capacitors in radial distribution systems using SPEA2 considering load uncertainty. *IET Gener. Transm. Distrib.* **2020**, *14*, 494–505. [CrossRef]
22. Sadeghian, O.; Oshnoei, A.; Kheradmandi, M.; Mohammadi-Ivatloo, B. Optimal placement of multi-period-based switched capacitor in radial distribution systems. *Comput. Electr. Eng.* **2020**, *82*, 106549. [CrossRef]
23. Das, S.; Das, D.; Patra, A. Operation of distribution network with optimal placement and sizing of dispatchable DGs and shunt capacitors. *Renew. Sustain. Energy Rev.* **2019**, *113*, 109219. [CrossRef]
24. de Araujo, L.R.; Penido, D.R.R.; Carneiro, S.; Pereira, J.L.R. Optimal unbalanced capacitor placement in distribution systems for voltage control and energy losses minimization. *Electr. Power Syst. Res.* **2018**, *154*, 110–121. [CrossRef]
25. Elsayed, A.M.; Mishref, M.M.; Farrag, S.M. Optimal allocation and control of fixed and switched capacitor banks on distribution systems using grasshopper optimisation algorithm with power loss sensitivity and rough set theory. *IET Gener. Transm. Distrib.* **2019**, *13*, 3863–3878. [CrossRef]
26. Gampa, S.R.; Jasthi, K.; Goli, P.; Das, D.; Bansal, R. Grasshopper optimization algorithm based two stage fuzzy multiobjective approach for optimum sizing and placement of distributed generations, shunt capacitors and electric vehicle charging stations. *J. Energy Storage* **2020**, *27*, 101117. [CrossRef]
27. Mirjalili, S. Dragonfly algorithm: A new meta-heuristic optimization technique for solving single-objective, discrete, and multi-objective problems. *Neural Comput. Appl.* **2015**, *27*, 1053–1073. [CrossRef]
28. Rajesh, P.; Shajin, F.H. Optimal allocation of EV charging spots and capacitors in distribution network improving voltage and power loss by Quantum-Behaved and Gaussian Mutational Dragonfly Algorithm (QGDA). *Electr. Power Syst. Res.* **2021**, *194*, 107049. [CrossRef]
29. Gholami, K.; Parvaneh, M.H. A mutated salp swarm algorithm for optimum allocation of active and reactive power sources in radial distribution systems. *Appl. Soft Comput.* **2019**, *85*, 105833. [CrossRef]
30. Mirjalili, S.; Gandomi, A.H.; Mirjalili, S.Z.; Saremi, S.; Faris, H.; Mirjalili, S.M. Salp Swarm Algorithm: A bio-inspired optimizer for engineering design problems. *Adv. Eng. Softw.* **2017**, *114*, 163–191. [CrossRef]
31. Ceylan, O.; Paudyal, S. Optimal capacitor placement and sizing considering load profile variations using moth-flame optimization algorithm. In Proceedings of the 2017 International Conference on Modern Power Systems (MPS), Cluj, Romania, 6–9 June 2017; pp. 1–6. [CrossRef]
32. Baimakhan O., Şenyüz H.; Sauchimov, A.; Ceylan, O. Optimal capacitor sizing and placement using dragonfly algorithm: A case study in kazakhstan. In Proceedings of the 12th Mediterranean Conference on Power Generation, Transmission, Distribution and Energy Conversion (MEDPOWER 2020), Paphos, Cyprus, 9–12 November 2020; pp. 208–212.
33. Abualigah, L.; Shehab, M.; Alshinwan, M.; Alabool, H. Salp swarm algorithm: A comprehensive survey. *Neural Comput. Appl.* **2020**, *32*, 11195–11215. [CrossRef]
34. Meraihi, Y.; Ramdane-Cherif, A.; Acheli, D.; Mahseur, M. Dragonfly algorithm: A comprehensive review and applications. *Neural Comput. Appl.* **2020**, *32*, 16625–16646. [CrossRef]
35. Abou El-Ela, A.A.; El-Sehiemy, R.A.; Kinawy, A.; Mouwafi, M.T. Optimal capacitor placement in distribution systems for power loss reduction and voltage profile improvement. *IET Gener. Transm. Distrib.* **2016**, *10*, 1209–1221. [CrossRef]
36. Mirjalili, S. Dragonfly Algorithm (DA) Source Codes (Version 1.0). Available online: https://seyedalimirjalili.com/da (accessed on 10 January 2022).
37. Mirjalili, S. Salp Swarm Algorithm (SSA) Source Codes (Version 1.0). Available online: https://seyedalimirjalili.com/ssa (accessed on 10 January 2022).